

Comparing and interpolating distributions on manifold

Nikolay H. Balov *

balov@stat.fsu.edu

December 7, 2021

Abstract

We are interested in comparing probability distributions defined on Riemannian manifold. The traditional approach to study a distribution relies on locating its mean point and finding the dispersion about that point. On a general manifold however, even if two distributions are sufficiently concentrated and have unique means, a comparison of their covariances is not possible due to the difference in local parametrizations. To circumvent the problem we associate a covariance field with each distribution and compare them at common points by applying a similarity invariant function on their representing matrices. In this way we are able to define distances between distributions. We also propose new approach for interpolating discrete distributions and derive some criteria that assure consistent results. Finally, we illustrate with some experimental results on the unit 2-sphere.

1 Introduction

The problem of comparing distributions defined on a non-Euclidean space or to be more specific, a Riemannian manifold, becomes increasingly important. A typical example of non-trivial manifold is the unit 2-sphere \mathbb{S}^2 , which is the domain of our experiments in this work. In this sense, our study has as

*Florida State University, Department of Statistics

main application problems from directional statistics, a branch of statistics dealing with directions and rotations in \mathbb{R}^3 .

Pioneers in the field are Fisher, R.A.(1953) and von Mises. In recent years directional statistics proved to be useful in variety of disciplines like shape analysis [26], geology, crystallography [24], bio-informatics [28] and data mining [4]. Most of the practitioners in these fields use parametric distributions to model directional data, like von Mises-Fisher distribution and Fisher-Bingham-Kent(FBK) distributions.

There are application areas however, where parametric models are insufficient. A recent example is provided by medical imaging community. In a new technique based on MRI and called High Angular Resolution Diffusion Imaging (HARDI), the data is represented by Orientation Distribution Functions (ODFs) which are nothing but discrete distributions on the unit 2-sphere. These distributions by their nature are multi-modal - they are not concentrated about a particular direction. They do not follow a parametric model and even if they do the eventual model would be too complicated to be efficient. Consequently, a non-parametric approach is more natural in processing ODFs.

In analysis of HARDI data researchers first have to solve the problem of registration between different volumes of ODFs, corresponding to the images of different subjects. For this purpose they need models and algorithms for interpolation between ODFs. Second, researchers are interested in comparing different groups of subjects using HARDI imaging. Usually, a statistical procedure is employed and hypotheses are tested. However, comparison between volumes requires comparison between corresponding ODFs and no standard method for this is available. A third problem in processing HARDI data is building connectivity paths for a given volume. Once again we need a consistent way to interpolate between ODFs in order to follow an optimal propagating direction.

There are no many choices for interpolation procedure beyond the simplest linear one. A recent alternative, using the square root representation of probability mass functions, was proposed by Srivastava(2007) and implemented in [9]. No existing solution though respects the geometry of the underlying domain.

In conclusion, we need more models and non-parametric procedures for comparing and interpolating distributions on the sphere and on Riemannian manifolds in general. Approaches that address the non-Euclidean nature of the random variables and provide adequate solutions. It is the main subject

of this paper to draw some new directions for searching of possible solutions.

What we propose basically is a generalization of the classical concept of covariance of distribution. We allow covariance to be defined with respect to any point of distribution domain and by doing so we try to workaround the problem of finding the mean point, which might not exist or be ambiguous. Also, since compact manifolds like \mathbb{S}^2 do not admit global parametrizations, we pay special attention to use the correct mathematical tool for describing the covariance. We not only point out to the well known fact that covariance can be viewed as a bi-linear operator and thus defined as a tensor, but specify the exact variance of this tensor. It is important to make a distinction between covariance tensor and metric tensor on manifold. A central observation in our approach is that at any point of the domain, the product of the metric and covariance tensors is a linear operator on the respected tangent space. We call it *covariance operator*. Collectively they form a field of operators. Then we introduce instruments, the so called similarity invariant functions, that can be used to study properties of these fields and to manipulate them.

After a formal introduction to the concept of covariance operators in section 2, we continue in section 3 with motivating examples showing the advantages of the new approach. We consider a two-sample location problem of the sphere and apply several classical non-parametric tests to solve it. Test statistics are based on projections defined by covariance operator fields.

In section 4 we consider the problem of interpolation between distributions on the sphere, and discuss and compare several alternatives. We also show some examples of interpolation between ODFs. The results are encouraging in the possibility of developing new applications for processing HARDI.

Although in all our experiments we stay on the unit sphere, the theoretical framework still holds on a general Riemannian manifold and this is one of its main strengths.

2 Covariance fields

2.1 Random variables on manifold

Let M be a Riemannian n -manifold, $q \in M$ and let Exp_q be the exponential map at q , $Exp_q : M_q \rightarrow M$. If M is complete, then the exponential map Exp_q is defined on the whole tangent space M_q . Throughout this paper for convenience we will assume that M is a complete Riemannian n -manifold,

although often that is not necessary.

There is a maximal open set $U(q)$ in M_p containing the origin, where Exp_q is a diffeomorphism. Then the set $\mathcal{U}(q) = Exp_q(U(q))$ is called maximal normal neighborhood of q . On this normal neighborhood the exponential map is invertible and let

$$Log_q = Exp_q^{-1} : \mathcal{U}(q) \rightarrow M_p$$

be its inverse, the so called log-map. Log_q is diffeomorphism on $\mathcal{U}(q)$. We adopt the notation $\vec{qp} = Log_qp$ in analogy to the Euclidean case, $M = \mathbb{R}^n$, where $Log_qp = p - q = \vec{qp}$.

In particular, for $M = \mathbb{S}^n$ the log-map has a closed-form expression

$$\vec{qp} = \frac{\cos^{-1} \langle p, q \rangle}{(1 - \langle p, q \rangle^2)^{1/2}} (p - \langle p, q \rangle q),$$

which greatly simplifies metric related operations on the unit sphere.

The Borel sets on M generated by the open sets on M form a σ -algebra $\mathcal{A}(M)$ on M . Any Riemannian manifold has a natural measure \mathcal{V} on $\mathcal{A}(M)$, called *volume measure*. In local coordinates x it is given by

$$dV(x) = \sqrt{|G_x|} dx,$$

where G_x is the matrix representation of the metric tensor, $|G_x|$ is its determinant and dx is the Lebesgue measure in \mathbb{R}^n .

Example 1 Consider the two sphere, \mathbb{S}^2 , parametrized in geographical coordinates (θ, ϕ) . Then the metric tensor is represented by

$$G_{(\theta, \phi)} = \begin{pmatrix} 1 & 0 \\ 0 & \cos^2(\theta) \end{pmatrix} \quad (1)$$

and the volume form is $V(\theta, \phi) = \cos(\theta) d\theta d\phi$.

A random variable X on M is any measurable function from a probability space $(\Omega, \mathcal{B}, \mathcal{P})$ to $(M, \mathcal{A}(M), \mathcal{V})$. The distribution function F of X is defined as

$$F(A) = \mathcal{P}(X^{-1}(A)), A \in \mathcal{A}(M).$$

If F satisfies

$$F(A) = \int_A f(p) dV(p), \forall A \in \mathcal{A}(M),$$

for almost everywhere continuous (w.r.t. \mathcal{V}) function f , then F is said to be absolute continuous (w.r.t. \mathcal{V}) and f is its density (*pdf*).

2.2 Intrinsic and Extrinsic mean and covariance

Let (M, ρ) be a metric space. The *Fréchet mean* set of a distribution F is the set of minimizers of $Q(q) = \int \rho^2(q, p) dF(p)$. It was introduced by Fréchet (1948). If M is a Riemannian manifold M with metric structure g , then the intrinsic mean of F , is the Fréchet mean of (M, d_g) , where d_g is the geodesic distance. Karcher(1977) considered the intrinsic mean on M and gave conditions for its existence and uniqueness. An alternative to intrinsic mean is the extrinsic one, which is obtained by embedding M into a higher dimensional Euclidean space. We point to the influential paper of Bhattacharya R. and Patrangenaru, V. (2005) where the properties of extrinsic and intrinsic means and their relation and asymptotic properties are considered in details.

Once a mean point (intrinsic or extrinsic) is specified, the covariance can be defined as usual after fixing a coordinate system about that point.

To compare two distributions one may first look at their intrinsic means. If they differ, the distributions differ, otherwise one may compare further their covariances at the common mean point. This approach however suffers from at least two drawbacks. First, if the population mean set is large, then the finite sample intrinsic mean will have substantial variance. That will diminish the power of any test for equality of means and more importantly, will inevitably require comparing covariances at different points. Second, the intrinsic mean, provided it exists and it is unique, and the covariance alone do not specify completely a distribution.

Thus, if we want to answer the problem of comparing distributions, we need a more informative structure that completely represents distributions and that is defined in coordinates free manner for seamless manipulation and comparison.

2.3 Covariance operators

Many parametric families of distributions can be defined as functions on linear operators. Consider for example the standard normal distribution in \mathbb{R}^n with density

$$f(x) \propto \exp\left(-\frac{1}{2}\|x - \mu\|^2\right),$$

where $\mu \in \mathbb{R}^n$ is its mean. Since $\|x - \mu\|^2 = \text{tr}((x - \mu)(x - \mu)')$ and the matrix $L(x) = (x - \mu)(x - \mu)'$ defines a linear operator

$$L(x)(u, v) = u' L(x) v = [u'(x - \mu)][(x - \mu)'v], u, v \in \mathbb{R}^n,$$

we can express the density by $f(x) \propto h(L(x))$, $h(T) := \exp(-\frac{1}{2}\text{tr}(T))$.

The von Mises-Fisher and FBK distributions [22] on the unit 2-sphere give us other such examples. For example, the latter is given by density

$$f(\mathbf{x}) = \frac{1}{c(\kappa, \beta)} \exp\{\kappa\gamma_1 \cdot \mathbf{x} + \beta[(\gamma_2 \cdot \mathbf{x})^2 - (\gamma_3 \cdot \mathbf{x})^2]\},$$

where γ_1, γ_2 and γ_3 are three points on \mathbb{S}^2 representing orthonormal directions in \mathbb{R}^3 . We have $f(x) \propto h(L_1(x), L_2(x), L_3(x))$, where

$$L_i(x) = G(x)(\overrightarrow{x\gamma_i})(\overrightarrow{x\gamma_i})',$$

are linear operators at the tangent space at $x \in \mathbb{S}^2$ and

$$h(T_1, T_2, T_3) = \exp(\kappa \cos(\text{tr}(T_1)) + \beta[\cos^2(\text{tr}(T_2)) - \cos^2(\text{tr}(T_3))]).$$

In fact, any $L : x \mapsto L(x)$ in the presented examples is a field of linear operators on tangential spaces. The concept we are going to introduce generalizes the above observations.

We return to a general Riemannian manifold M with metric G . Fix a point $q \in M$. Recall that the metric $G(q)$ is a co-variant 2-tensor at M_q , while the quantity $(\overrightarrow{q\hat{p}})(\overrightarrow{q\hat{p}})'$ is a contra-variant 2-tensor at M_q . The contraction of their tensor product, $G(q)(\overrightarrow{q\hat{p}})(\overrightarrow{q\hat{p}})'$, is a (1,1)-tensor, which is nothing but a linear operator at M_q .

Now the idea becomes clear. For a distribution F on M , a linear operator at M_q can be obtained by taking the expectation of $G(q)(\overrightarrow{q\hat{p}})(\overrightarrow{q\hat{p}})'$, $p \sim F$.

From now on we will use the standard notation $T^2(M_q)$ for co-variant 2-tensors on M_q , $T_2(M_q)$ for contra-variant 2-tensors on M_q and $T_1^1(M_q)$ for bi-linear operators on M_q .

Definition 1 Let $r : \mathbb{R}^+ \rightarrow \mathbb{R}^+$ be a continuous function. Covariance of distribution F on M at point $q \in M$ is defined by

$$\Sigma(q) = \int_{\mathcal{U}(q)} (\overrightarrow{q\hat{p}})(\overrightarrow{q\hat{p}})' r(\|\overrightarrow{q\hat{p}}\|) dF(p) \quad (2)$$

and $\Sigma : q \mapsto \Sigma(q) \in T_2(M_q)$ is called covariance field of F .

With $r = 1$ we obtain the generic covariance field associated with F and this is the default choice.

As noted above, $G(q)\Sigma(q)$ is a linear operator on M_q , which we call *covariance operator*. Hence, $G\Sigma$ is a field of linear operators on M . With respect to

a coordinate system x at q , $G(q)\Sigma(q)$ is represented by a symmetric and positive definite matrix $G_x\Sigma_x$, where G_x and Σ_x are the representations of $G(q)$ and $\Sigma(q)$. In other words, $G\Sigma$ is a field of symmetric and positive definite operators on M .

If $v \in M_q$ has components v_x with respect to x , we define

$$(G(q)\Sigma(q))v := \Sigma_x G_x v_x$$

and

$$\langle v, (G(q)\Sigma(q))v \rangle := v'_x G_x \Sigma_x G_x v_x.$$

One can check that indeed the last quantity is invariant to coordinate change at q .

It is worth to mention that for a covariance field Σ on M , Σ^{-1} is also symmetric and positive definite and when it is differentiable, Σ^{-1} introduce a new Riemannian metric on M .

If Σ_1 and Σ_2 are two covariance fields on M , then $\Sigma_1\Sigma_2^{-1}$ is a field of linear operators, i.e. for any $q \in M$, $\Sigma_1(q)\Sigma_2^{-1}(q) \in T_1^1(M_q)$.

On a complete Riemannian manifold, the problem of minimizing the trace of the default covariance field is equivalent to the problem of finding the intrinsic mean of F , i.e.

$$\mu = \operatorname{argmin}_{q \in M} \left\{ \int_{\mathcal{U}(q)} \operatorname{tr}(G(q)(\vec{qp})(\vec{qp})') dF(p) = \int_M d_g^2(q, p) dF(p) \right\}.$$

2.4 Similarity invariants

Let Sym_n^+ denote the space of symmetric and positive definite matrices. Since this is the representation domain for covariance operators it is of obvious importance for us. Sym_n^+ attracted the attention of many researchers in the recent years due to its non-Euclidean nature and consequently, the variety of research opportunities it provides. For the purposes of Diffusion Tensor Imaging, Fletcher, P. T., Joshi, S., (2007) and Pennec. X., Fillard, P., Ayache, N (2006) proposed the use of *affine invariant* distance, while Arsigny, V., Fillard, P., Pennec X., and Ayache, N. (2007) proposed the so called log-Euclidean distance. A good survey of the available distances and estimators in Sym_n^+ along with new ones is provided by Dryden, I., Koloydenko, A., and Zhou, D., (2008). We aim a more general treatment of Sym_n^+

and instead of dealing with specific matrix functions we define a class of invariants. What particular member of this class should be used is application problem specific choice.

Two matrices $A, B \in Sym_n^+$ are said to be similar if

$$A = X^{-1}BX, \text{ for } X \in GL_n.$$

Matrix representations of linear operators are similar and thus, this fact holds for the representations of $G\Sigma$ and $\Sigma_1\Sigma_2^{-1}$. Next we define an important class of functions that respect similarity.

Definition 2 A similarity invariant function on Sym_n^+ is any continuous bi-variate h that satisfies

$$(i) \ h(AXA', AYA') = h(X, Y), \forall X, Y \in Sym_n^+ \text{ and } A \in GL_n.$$

It is a non-negative with a unique root if

$$(ii) \ h(X, Y) \geq 0, \forall X, Y \in Sym_n^+ \text{ and } h(X, Y) = 0 \iff X = Y.$$

Moreover, h is called similarity invariant distance, if in addition to (i) and (ii) also satisfies

$$(iii) \ h(X, Y) + h(Y, Z) \geq h(X, Z), \forall X, Y, Z \in Sym_n^+.$$

Below we list several examples of similarity invariant function we use in our experiments.

1. For a fixed $Z \in Sym_n^+$, the similarity invariant

$$h_{trdif}(X, Y; Z) = |(tr(Z^{-1}X - Z^{-1}Y))|,$$

satisfies (iii) but not (ii). Default choice will be $Z = G^{-1}$, the inverse of the metric tensor representation.

2. The second one is sometimes referred as *affine-invariant distance* in Sym_2^+ , see for example [29], [15], [5], [13] and [30], and it is defined by

$$h_{trln2}(X, Y) = \{tr(\ln^2(XY^{-1}))\}^{1/2}, X, Y \in Sym_2^+.$$

Actually, h_{trln2} is not a unique choice for a distance in Sym_2^+ .

3. Log-likelihood function gives us another choice for h ,

$$h_{lik}(X, Y) = \text{tr}(XY^{-1}) - \ln|XY^{-1}| - n.$$

It satisfies (i) and (ii) but it fails to satisfy the triangular inequality.

4. Another interesting choice for h is

$$h_{lnpr}(X, Y) = \{\ln(\text{tr}(XY^{-1})\text{tr}(YX^{-1}))\}^{1/2},$$

that satisfies (iii) and 'almost' satisfies (ii): $h_{lnpr}(X, Y) = 0 \iff X = cY$, for $c > 0$.

The concept of covariance fields can be used for measuring the difference between distributions on M . Let f and g be two densities on M and $\Sigma[f]$ and $\Sigma[g]$ be their respected covariance fields.

For a non-negative $h \in \mathcal{SLM}(n)$ we define

$$d_h(f, g) := \int_M h(\Sigma[f](p), \Sigma[g](p)) dV(p). \quad (3)$$

When M is a compact, the above integral is well defined and finite. Moreover, if $h(X, Y)$ is a distance function on Sym_n^+ , then d_h will be a distance in the space of densities on M .

Equation (3) gives a very general but impractical way to compare distributions due to the fact that the integration domain is the whole manifold. For application purposes however, one may restrict to a smaller domain or perform the comparison on discrete set of points which are of particular interest.

3 Two-sample location problem on \mathbb{S}^2

In this section we make an application of covariance operators to non-parametric distribution comparison. It will serve more illustration purposes rather than strong application ones. The goal is to provide motivating examples showing the new opportunities provided by the proposed covariance structure. We choose to apply simple procedures, as Wilcoxon signed rank and rank sum tests, in order to have a good look and intuition of what happens.

Let $\{p_{i,1}\}_{i=1}^m$ and $\{p_{i,2}\}_{i=1}^m$, be random samples from distributions F_1 and F_2 on \mathbb{S}^2 , respectively, and the two samples be independent of each other.

Fix a point $q \in M$ and define

$$\eta_i^1 = G(q)(\overrightarrow{qp_{i,1}})(\overrightarrow{qp_{i,1}})', \eta_i^2 = G(q)(\overrightarrow{qp_{i,2}})(\overrightarrow{qp_{i,2}})'$$

Using tensor notation we can write $\eta_i^l \in T_1^1(\mathbb{S}_q^2)$. The respective sample covariance operators at q are

$$\hat{L}^1(q) = \frac{1}{m} \sum_{i=1}^m \eta_i^1 \text{ and } \hat{L}^2(q) = \frac{1}{m} \sum_{i=1}^m \eta_i^2.$$

We call q *observation point* and basically, what we are going to show is how its choice influences the inference about F_1 and F_2 .

Fix a tangent vector $v \in \mathbb{S}_q^2$ and consider following (ordinary) random variables

$$\xi_i^1(v) = \langle v, \eta_i^1(v) \rangle_q \text{ and } \xi_i^2(v) = \langle v, \eta_i^2(v) \rangle_q,$$

where $\langle \cdot, \cdot \rangle_q$ is the dot product in the tangent space \mathbb{S}_q^2 .

Definition 3 We say that F_1 and F_2 have the same location w.r.t. $q \in \mathbb{S}^2$ and write $F_1 \cong_q F_2$ if for any $v \in \mathbb{S}_q^2 \cong \mathbb{R}^2$, random variables

$$\xi^l(v) = \langle v, (G(q)(\overrightarrow{qX_l})(\overrightarrow{qX_l})') \rangle(v) >_q, X_l \sim F_l, l = 1, 2$$

have the same median.

Under the hypothesis $H_0 : F_1 \cong_q F_2$, for any v , $\xi_i^1(v)$ and $\xi_i^2(v)$ are random samples from distributions with equal median.

To test H_0 we propose two procedures based on the Wilcoxon signed rank test, [17], page 36. Let $T_{xi}(v)$ ¹ be the signed rank statistics based on $\xi_i(v)$'s and $T_{xi} = \max\{T_{xi}(v), v \in \mathbb{R}^2\}$. Then we reject H_0 when T_{xi} is sufficiently large.

The second test is based on T_d , the Wilcoxon signed rank statistics for the distances

$$d_i^1 = \text{tr}(\eta_i^1(v)) = d^2(q, p_{i,1}) \text{ and } d_i^2 = \text{tr}(\eta_i^2(v)) = d^2(q, p_{i,1}),$$

where d^2 stands for the spherical distance, $d^2(q, p) = \cos^{-1}(\langle q, p \rangle)$.

¹ $T_{xi} = \sum_i r_i s_i$, where for $z_i = \xi_i^1 - \xi_i^2$, $s_i = 1_{\{z_i > 0\}}$ and r_i are the ranks of $|z_i|$.

If we choose an orthonormal basis $\{v_s\}_{s=1}^2$ of $\mathbb{S}_q^2 \cong \mathbb{R}^2$ and define

$$\xi_{i,s}^1 = \langle v_s, \eta_i^1 v_s \rangle_q \quad \text{and} \quad \xi_{i,s}^2 = \langle v_s, \eta_i^2 v_s \rangle_q,$$

then the following holds: for any $i = 1, \dots, m$ and $l = 1, 2$

$$\sum_{s=1}^2 \xi_{i,s}^l = \sum_{s=1}^2 \langle v_s, \overrightarrow{qp_{i,l}} \rangle^2 = \|\overrightarrow{qp_{i,l}}\|^2 = \text{tr}(\eta_i^l(v)) = d_i^l. \quad (4)$$

It is clear that if $\xi^1(v_1)$ and $\xi^2(v_1)$ have the same median and $\xi^1(v_2)$ and $\xi^2(v_2)$ also have the same median, then $\xi^1(v)$ and $\xi^2(v)$ will have the same median for every v .

$\{d_i^1\}_i$ and $\{d_i^2\}_i$ are samples from marginals of F_1 and F_2 , which under the null hypothesis have the same location. As distances, they are invariant to rotation of the samples $p_{i,l}$ on the sphere. On the other hand, for any l , $\{\xi_{i,1}^l\}_i$ and $\{\xi_{i,2}^l\}_i$ follow two marginal distributions that can be considered projections of F_l onto two orthogonal axes. As such they form more discriminating set of variables than $\{d_i^l\}_i$.

These observations motivate the following procedure for testing H_0 .

Test Procedure 1 *Let $\{p_{i,l}\}_{i=1}^m$, $l=1,2$ be two random samples, independent of each other.*

1. Find the operators η_i^1 and η_i^2 and set

$$\hat{L}(q) = \hat{L}^1(q) - \hat{L}^2(q) = \frac{1}{m} \sum_{i=1}^m \eta_i^1 - \frac{1}{m} \sum_{i=1}^m \eta_i^2.$$

2. Let λ_s and v_s be the eigenvalues and eigenvectors of $\hat{L}(q)$.

Set $\xi_{i,s}^l = \langle v_s, \eta_i^l v_s \rangle_q$.

3. Calculate statistics $T_{xi,s}$ based on $\xi_{i,s}^l$ and set

$$T_{xi} = \max\{T_{xi,1}, T_{xi,2}\}.$$

4. Choose a significance level α . If $pval(T_{xi}) < \alpha/2$ ², reject H_0 .

²We apply Bonferroni correction for the p-value.

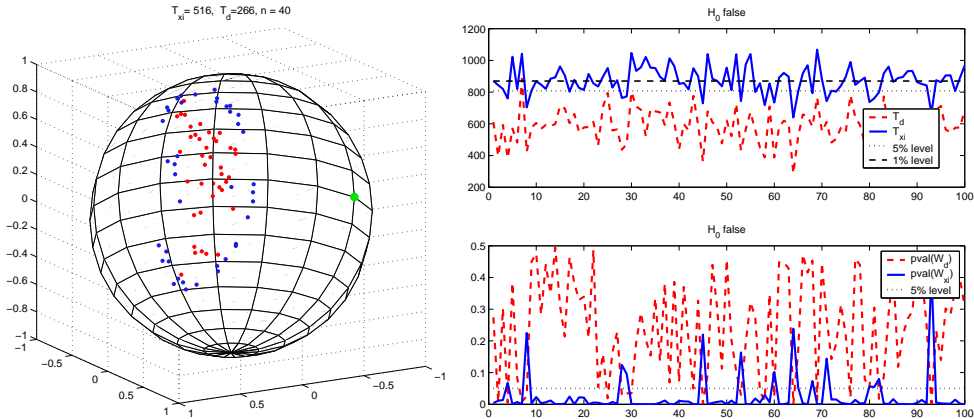


Figure 1: Testing $H_0 : F_1 \cong_q F_2$ when H_0 is false. Sample examples from F_1 (red) and F_2 (blue) are given in the left. Observation point q , shown in green, is fixed and equals distribution parameter μ . Top right plot shows T_{xi} and T_d statistics along with 1 and 5 percentile lines, while the bottom right plot shows W_{xi} and W_d by their p-values. Test procedure 1 is run 100 times with sample size of 50. T_{xi} clearly outperforms T_d statistics by rejecting the null hypothesis most of the time and the same is true for W_{xi} versus W_d .

We also employ the rank sum test (Wilcoxon, Mann and Whitney), [17], page 106, to compare the performance of ξ_i^l and $d_{i,l}$ random variables. For the statistics W_{xi} ³ and W_d , we calculate corresponding p-values using large sample approximation. The second test procedure is the same as the first one but uses W instead of T statistics.

Note that if F_2 distribution is a rotation of F_1 about q , then the type II error of T_d statistics will be 1, i.e. the power will be 0.

The way of choosing the basic vectors v_s of \mathbb{S}_q^2 resembles the Principal Component Analysis (PCA) of the operator $\hat{L}(q)$ and its derivatives like Principal Geodesic Analysis (PGA), introduced by Fletcher, 2004. In the standard setup, PCA is applied on the covariance defined at the (extrinsic or intrinsic) mean point. However, not only the existence of a mean is not guaranteed, but its properties may not be optimal in the context of the test statistic. In contrast, in our approach we allow freedom of choosing the observation point q according to a criteria favoring that statistic.

Figures 1 and 2 show some experimental results using the proposed pro-

³ $W_{xi} = \sum_i r_i$, where for r_i are the ranks of ξ_i^1 in the joint sample $\{\xi_i^1, \xi_i^2\}$.

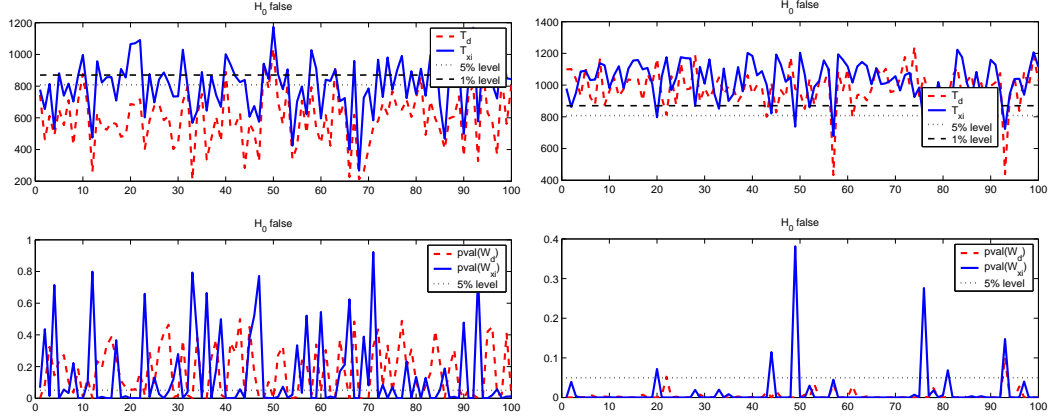


Figure 2: Performance of T and W statistics when the observation point q varies. In the left plot q is chosen uniformly on the sphere. The experiment confirms a clear advantage for T_{x_i} . In the right plot preference is given to those observation points for which $tr^2(\hat{L})$ is large. Now T_d is on a par to T_{x_i} with both being very high. Corresponding W_d and W_{x_i} also have very significant p-values.

cedures for testing $H_0 : F_1 \cong_q F_2$. We consider a family of distributions given by density

$$f(p; a, \mu) \propto \exp(-(\text{tr}(G(\mu)(\vec{\mu}\vec{p})(\vec{\mu}\vec{p}))^2 - a)^2) \quad (5)$$

where μ is a fixed point (not to be mistaken as a mean) and a is a parameter. Top plots show Wilcoxon sign rank statistics T , while bottom plots show rank sum statistics W . As we see in figure 2 left, where the observation point q varies uniformly on \mathbb{S}^2 , for the majority of positions, T_{x_i} and W_{x_i} achieve higher p-values than T_d and W_d . This result is not isolated and can be repeated for a great variety of distributions besides (5).

How the choice of observation point q affects the relative performance of T and W statistics? We have that

$$d_i^1 - d_i^2 = \sum_{s=1}^2 (\xi_{i,s}^1 - \xi_{i,s}^2) \text{ and } \frac{1}{m} \sum_{i=1}^m (\xi_{i,s}^1 - \xi_{i,s}^2) = \lambda_s,$$

thus

$$\frac{1}{m} \sum_{i=1}^m (d_i^1 - d_i^2) = \sum_s \lambda_s.$$

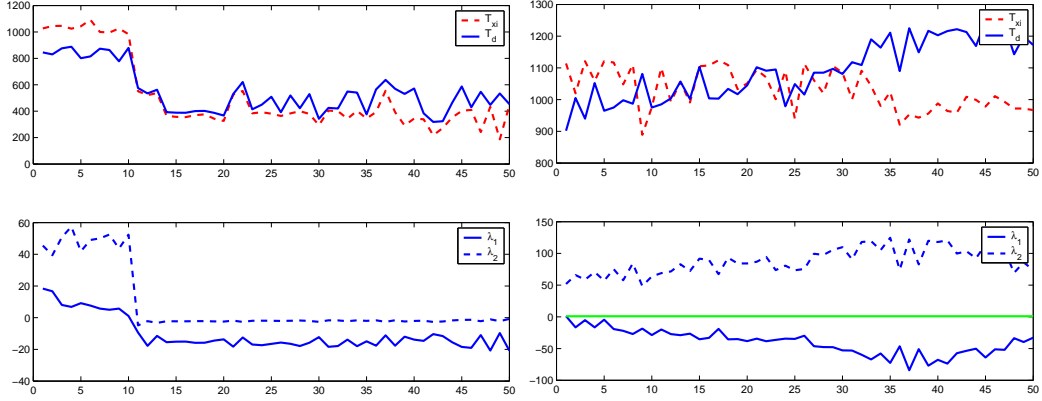


Figure 3: Comparing the performances of T_{xi} and T_d statistics (top) for a fixed pair of samples by varying the observation point. Samples are drawn from (5). Observation points are ordered decreasingly in $\det(\hat{L}(q))$ in the left plot and decreasingly in $tr^2(\hat{L}(q))$ in the right. The bottom plot shows the eigenvalues of $\hat{L}(q)$. We note that T_d is the larger statistics and thus, has lower p-values, only when both eigenvalues are strictly positive.

Therefore, if all λ_s are of equal sign, the absolute value of the sample expectation of $(d_i^1 - d_i^2)$ will be higher than that of $(\xi_{i,s}^1 - \xi_{i,s}^2)$, for all s . In case when the eigenvalues are of different signs the reverse is expected, the absolute value of the sample expectation of $(\xi_{i,s}^1 - \xi_{i,s}^2)$ for the maximal $|\lambda_s|$ will be higher than that of $(d_i^1 - d_i^2)$, which means that T_{xi} is expected to be higher than T_d . Of course these considerations are only approximate because the tests for T and W statistics are based on assumptions on the medians not on the means. Nevertheless, we may take the above as a general observation that can be made more formal and rigorous using other appropriate statistical tests.

We provide some experimental evidence confirming the above expectations. For comparison the performance of T_{xi} and T_d we use $\det(\hat{L}(q))$. We expect for T_d to benefit from positive values of $\det(\hat{L}(q))$ and indeed this is the case as seen in figure 3 left. There, for a fixed pair of samples, we calculate and compare T_{xi} and T_d statistics at 50 observation points on the sphere. Then we sort the results such that $\det(\hat{L}(q))$ decreases. In the far left, both λ_1 and λ_2 are positive, which leads to a clear advantage for T_d . Once the sign of $\det(\hat{L}(q))$ goes negative, the situation reverses.

We also expect that at observation points with high values of $tr^2(\hat{L})$, all

statistics to be strong in rejecting a false null hypothesis. Some evidence confirming this is shown in figures 2 right and 3 right. $tr^2(\hat{L})$ is probably the simplest statistics that measures the difference between the two samples and it is in fact, an application of the similarity invariant function h_{trdif} as defined in section 2.2.

One can show that \hat{L} is a continuous field of linear operators on \mathbb{S}^2 (the proof is beyond the scope of the paper). Therefore, if there exists a point q with $det(\hat{L}(q)) < 0$, then that sign is negative on non-vanishing area. Only when samples $p_{i,l}$ collectively are highly concentrated, the area S_+ where $det(\hat{L}(q)) > 0$ will dominate over S_- , the area where $det(\hat{L}(q)) < 0$. In case when H_0 is false, we expect that $S_+ < S_-$.

Figure 4 gives another useful way to visualize the sample operator \hat{L} at different observation points. By choosing a point q , one can draw the projections $\langle v, \eta_i^l(v) \rangle_q$ for a set of directions v spanning a circle to obtain the so called sample profile.

In conclusion, choosing an observation point for comparing locations of two distributions is an important issue since not all positions provide same test performance. Position optimality depends on the statistic applied on the covariance operator. For the projection based statistics we used as examples, optimal observation points can be chosen by maximizing the squared trace of the difference of the covariance operators.

We also showed that distance based statistics have limited performance and in general, employing the whole covariance structure is beneficial.

We also note that most of the presented results do not depend on the specific geometry of the unit sphere and still hold on a general Riemannian manifold.

4 Interpolation of discrete distributions on \mathbb{S}^2

The second application of the covariance operators we are going to consider is interpolation between discrete distributions on the unit sphere. We suppose that the distributions are defined on a common domain - a fixed set of points on the sphere. The approach we propose is first, to generate an interpolated field based on the covariance fields of the initial distributions and second, to find a probability mass function which covariance field is close to the interpolated one. Closeness is measured using a suitable similarity invariant function. Covariance fields are also considered discrete ones - they are

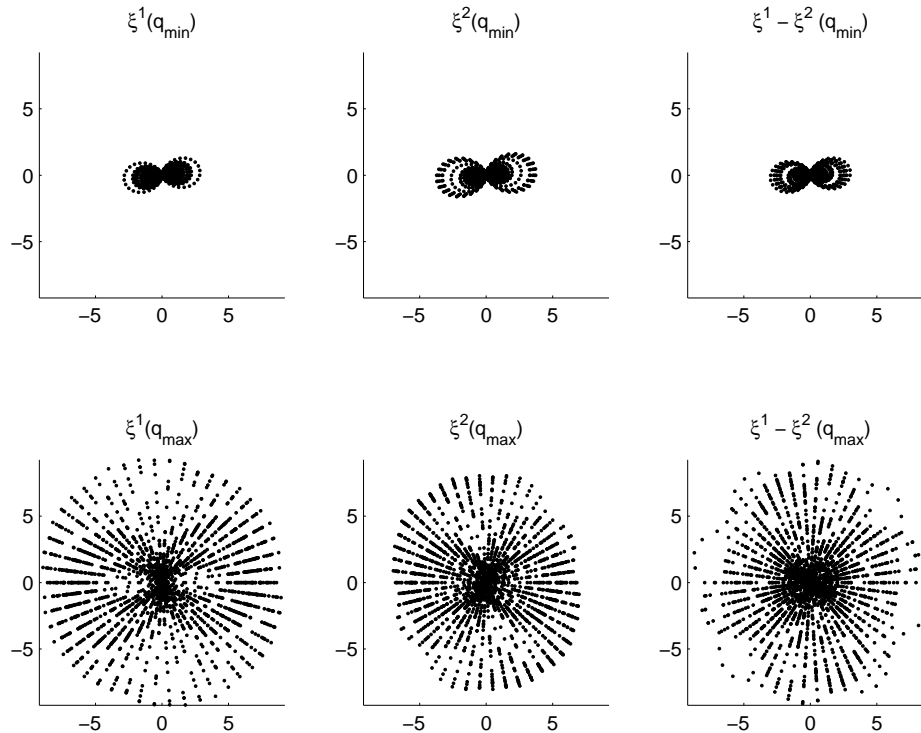


Figure 4: Two samples of size 50 are drawn from $f(p; 0.2)$ and $f(p; 0.3)$ as given by (5). Points q_{\min} and q_{\max} are chosen to minimize and maximize $tr^2(\hat{L}_1 - \hat{L}_2)$. Shown are sample profiles and their difference (right) at these points, defined by the projections $\xi = \langle v, \eta(v) \rangle$ along 50 directions v spanning uniformly $[0, 2\pi]$. Profiles of ξ^1 and ξ^2 are concentrated and look similar at q_{\min} , but are diffused and very different at q_{\max} . These plots visualize clearly the difference between two extreme observation points.

defined on a finite set of observation points. With a fixed coordinate system at each observation point, not necessarily a global one, the covariance field is represented by a set of matrices. As always, we are going to use the tensor notation to guarantee a coordinate free approach.

Let $\{p_i\}_{i=1}^k$ and $\{q_i\}_{i=1}^k$ be two sets of k points on \mathbb{S}^2 . The first set is the distribution domain. The second one is the observation set. Hereafter, a discrete mass function (pmf) is any k -vector f , such that $f = \{f_i = f(p_i) \geq 0\}_{i=1}^k$ and $\sum_{i=1}^k f_i = 1$. We write $f \in P_k^+$, where P_k^+ denotes the compact k -simplex.

The number of observation points may be in fact less than k , the size of the *pmfs*. However, with a smaller observation set one may lose the uniqueness and the continuity of an estimation. Particular geometric configurations also lead to the same result and one has to check carefully the consistency conditions corresponding to the problem.

The covariance field of $f \in P_k^+$ at q_j is defined as

$$\Sigma[f]_j := \Sigma[f](q_j) = \sum_{i=1}^k (\overrightarrow{q_j p_i})(\overrightarrow{q_j p_i})' r(\|\overrightarrow{q_j p_i}\|) f(p_i),$$

where

$$\overrightarrow{q_j p_i} = \frac{\cos^{-1} \langle p_i, q_j \rangle}{(1 - \langle p_i, q_j \rangle^2)^{1/2}} (p_i - \langle p_i, q_j \rangle q_j).$$

We use either $r = 1$ or

$$r(t) = \left(1 - \frac{\pi}{2t}\right)^2. \quad (6)$$

The second choice is known to be optimal on \mathbb{S}^2 in the class of functions $r_a(t) = \left(1 - \frac{a}{t}\right)^2$ because it minimizes the maximum of $\text{tr}(G\Sigma(q))$.

Let $f^s, s=1, \dots, m$, be a collection of *pmfs* and

$$\{C_j^s = \Sigma[f^s]_j\}_{j=1}^k, s = 1, \dots, m,$$

be their covariance fields.

For a non-negative similarity invariant function h , we define

$$d_h(f, f^s) := \sum_{j=1}^k h(\Sigma[f]_j, C_j^s), s = 1, \dots, m. \quad (7)$$

For $\alpha \in P_m^+$, i.e. $\alpha = \{\alpha_s\}_{s=1}^m$, such that $\alpha_s \geq 0$ and $\sum_s \alpha_s = 1$, we define the functional

$$H(f; \alpha) := \sum_{s=1}^m \alpha_s d_h(f, f^s). \quad (8)$$

Then we formulate the following optimization problem: find a probability mass function \hat{f} such that

$$\hat{f}(\alpha) = \operatorname{argmin}_f H(f; \alpha). \quad (9)$$

Below we show some results regarding the consistency of the estimators (9).

Lemma 1 *Let $h \in \mathcal{SIM}(n)$, $\alpha_s \in P_M^+$ and $f^s \in P_k^+$. If $\alpha_s \rightarrow \alpha_0$ and $f^s \rightarrow f^0$ (in L_2 norm), then*

$$H(f^s, \alpha_s) \rightarrow H(f^0, \alpha_0).$$

Proof. Observe that

$$|H(f^s; \alpha_s) - H(f^0; \alpha_0)| \leq |H(f^s; \alpha_s) - H(f^s; \alpha_0)| + |H(f^s; \alpha_0) - H(f^0; \alpha_0)|.$$

Since $H(f; \alpha_0)$ is continuous in f , the second term above goes to zero. The first term is bounded by

$$|H(f^s; \alpha_s) - H(f^s; \alpha_0)| \leq \|\alpha_s - \alpha_0\|_{L_2} \max_{j,m} h(\Sigma[f]_j, C_j^s).$$

The sets $\{\Sigma[f]_j | f \in P_k^+\}$ are compact in Sym_n^+ and h is continuous, therefore $\max_{j,m} h(\Sigma[f]_j, C_j^s) = C < \infty$ and

$$H(f^s; \alpha_s) \rightarrow H(f^s; \alpha_0).$$

□

For a sequence α_s , define $\hat{f}^s = \operatorname{argmin}_f H(f; \alpha_s)$. We have the following

Lemma 2 *If $h \in \mathcal{SIM}(n)$ and $\alpha_s \rightarrow \alpha_0$, then*

$$H(\hat{f}^s, \alpha_s) \rightarrow H(\hat{f}^0, \alpha_0). \quad (10)$$

Proof. Since P_k^+ is a compact any sub sequence of f^s has a point of convergence in P_k^+ . Without loss of generality we may assume that $\hat{f}^s \rightarrow g \in P_k^+$. Accounting for the minimizing properties of \hat{f} and applying lemma 1 we can write

$$H(\hat{f}^0, \alpha_s) \geq H(\hat{f}^s, \alpha_s) \rightarrow H(g, \alpha_0) \geq H(\hat{f}^0, \alpha_0).$$

Because of $H(\hat{f}^0, \alpha_s) \rightarrow H(\hat{f}^0, \alpha_0)$ we have (10). \square

Unfortunately, (10) is not enough to claim that $\hat{f}^s \rightarrow \hat{f}^0$. However, if $H(f; \alpha_0)$ has a well separated minimum at \hat{f}^0 we indeed have the wanted consistency.

Corollary 1 $\hat{f}(\alpha)$ is continuous at all α for which $H(f, \alpha)$ has a well separated (global) minimum.

Another problem is how to find the global minimum \hat{f} of $H(f; \alpha)$, provided it is unique. We know that the minimum is easily found in case of convex function H , by gradient descent algorithm for example. Moreover, the convexity of $H(f; \alpha_0)$ in P_k^+ guarantees the well separability of its minimum and that gives us the desired consistency.

Proposition 1 If $\alpha_s \rightarrow \alpha_0$ and $h \in \mathcal{SLM}(n)$ is such that $H(f; \alpha_0)$ is convex in P_k^+ , then

$$\hat{f}^s \rightarrow \hat{f}^0. \tag{11}$$

Proof. Suppose the contrary of (11), that there exists $g \in P_k^+$, and sub sequence $\hat{f}^s \rightarrow g$, such that $\|\hat{f}^0 - g\| > 0$. Then $H(g; \alpha_0) > H(\hat{f}^0; \alpha_0)$ by the separability of the minimum. But $H(\hat{f}^s; \alpha_s) \rightarrow H(g; \alpha_0)$ by lemma 1 and $H(\hat{f}^s; \alpha_s) \rightarrow H(\hat{f}^0; \alpha_0)$ by lemma 2, which imply $H(g; \alpha_0) = H(\hat{f}^0; \alpha_0)$. The contradiction proves the claim. \square

4.1 Linear Interpolation

Consider first one of the simplest similarity invariant functions $h_{trdif}^2(\cdot, \cdot; G^{-1})$. The corresponding optimization functional is

$$H_{trdif}(f, \alpha) = \sum_{s=1}^m \alpha_s \sum_{j=1}^k tr^2(G(q_j)\Sigma[f]_j - G(q_j)C_j^s)$$

Denote $a_{ij} = \text{tr}(G(q_j)(\overrightarrow{q_j p_i})(\overrightarrow{q_j p_i})') = d^2(q_j, p_i)$ and $c_j^s = \text{tr}(G(q_j)C_j^s)$, then

$$H_{\text{trdif}}(f, \alpha) = \sum_{s=1}^m \alpha_s \sum_{j=1}^k \left(\sum_i a_{ij} f_i - c_j^s \right)^2.$$

We have

$$\frac{\partial H_{\text{trdif}}}{\partial f_i} = 2 \sum_{s=1}^m \alpha_s \sum_{j=1}^k a_{ij} \left(\sum_l a_{lj} f_l - c_j^s \right).$$

The second partial derivatives are

$$\frac{\partial^2 H_{\text{trdif}}}{\partial f_i \partial f_l} = 2 \sum_{s=1}^m \alpha_s \sum_{j=1}^k a_{ij} a_{lj}$$

Let $w = \{w_i\} \in \mathbb{R}^k$, then

$$\sum_{i,l} w_i w_l \frac{\partial^2 H_{\text{trdif}}}{\partial f_i \partial f_l} = 2 \sum_{s=1}^m \alpha_s \sum_{j=1}^k \left(\sum_{i=1}^k w_i a_{ij} \right)^2 \geq 0.$$

Therefore, if the matrix $A = \{a_{ij}\}_{i=1,j=1}^{k,k}$ is of full rank k , then H_{trdif} is convex in P_k^+ . Moreover, the optimal solution of (9) satisfies

$$\sum_i a_{ij} f_i = \sum_{s=1}^m \alpha_s c_j^s, j = 1, \dots, k,$$

with a unique solution

$$\hat{f} = \sum_{s=1}^m \alpha_s f^s,$$

since for every s and j , $\sum_i a_{ij} f_i^s = c_j^s$.

Thus, we showed the following

Proposition 2 *If the matrix A has full rank, $\text{rank}(A) = k$, then the linear interpolation is the unique solution of the optimization problem (9) for H_{trdif} .*

4.2 Non-Linear Interpolations

Consider similarity invariant function h_{trln2} and corresponding optimization functional H_{trln2}

$$H_{\text{trln2}}(f; \alpha) = \sum_{s=1}^m \alpha_s \sum_{j=1}^k \text{tr}(\ln^2(\Sigma[f]_j(C_j^s)^{-1})).$$

The value of $H_{trln2}(f)$ is small when $G(q_j)\Sigma[f]_j$ is close to covariance operators $G(q_j)C_j^s$ for all j and s . This is a much stronger condition than the requirement for their traces to be close as in the problem of minimizing H_{trdif} . Consequently the minimum of $H_{trln2}(f)$, in general, will be strictly positive and the optimal pmf will be different from the linear interpolation.

Experiments show great improvement in convergence of gradient descend algorithm for problem (9), when instead of the generic covariance one uses the second choice (6).

Define the operators

$$Z_{ij}^s = (\overrightarrow{q_j p_i})(\overrightarrow{q_j p_i})'(1 - \frac{\pi}{2\|\overrightarrow{q_j p_i}\|})^2(C_j^s)^{-1}$$

and set $Y_j^s = \sum_i f_i Z_{ij}^s$. The gradient of H_{trln2} is

$$\nabla H_{trln2}(f, \alpha) = \{f_i \sum_{s=1}^m \alpha_s \sum_{j=1}^k \frac{tr(\ln(Y_j^s)Z_{ij}^s)}{tr(Z_{ij}^s)}\}_{i=1}^k.$$

The optimization problem (9) is solved by gradient descent algorithm, which shows relatively fast convergence, unfortunately not always to the global minimum, because $H_{trln2}(f, \alpha)$ is not convex in $f \in P_k^+$.

Log-likelihood function gives us another choice for H ,

$$\begin{aligned} H_{lik}(f; \alpha) &= \sum_{s=1}^m \alpha_s \sum_{j=1}^k \{tr(\Sigma[f]_j(C_j^s)^{-1}) - \ln|\Sigma[f]_j(C_j^s)^{-1}| - n\} = \\ &= \sum_{s=1}^m \alpha_s \sum_{j=1}^k \{tr(Y_j^s) - \ln|Y_j^s| - n\}. \end{aligned}$$

The gradient of H_{lik} is

$$\nabla H_{lik}(f; \alpha) = \{f_i \sum_{s=1}^m \alpha_s \sum_{j=1}^k \frac{tr((Y_j^s - I_n)Z_{ij}^s)}{tr(Z_{ij}^s)}\}_{i=1}^k.$$

Note that h_{lik} is neither symmetric nor satisfies the triangular inequality, but its importance is determined by the relation to normal distributions and its analytical properties. Define the matrix

$$B = \{b_{ij} = (d(q_j, p_i) - \frac{\pi}{2})^2\}_{i=1, j=1}^{k, k}.$$

Proposition 3 *If B has full rank, $\text{rank}(B) = k$, then for all α , $H_{lik}(f; \alpha)$ is a convex function in P_k^+ .*

Proof. We have

$$\frac{\partial H_{lik}}{\partial f_i} = \sum_{s=1}^m \alpha_s \sum_{j=1}^k \text{tr}(Z_{ij}^s - Z_{ij}^s (Y_j^s)^{-1}).$$

and

$$\frac{\partial^2 H_{lik}}{\partial f_i \partial f_l} = \sum_{s=1}^m \alpha_s \sum_{j=1}^k \text{tr}(Z_{ij}^s (Y_j^s)^{-1} Z_{lj}^s (Y_j^s)^{-1}).$$

We want to show that the matrix of second partial derivatives is positive definite. Let $w = \{w_i\} \in \mathbb{R}^k$ and $w \neq 0$, then

$$\sum_{i,l} w_i w_l \frac{\partial^2 H_{lik}}{\partial f_i \partial f_l} = \sum_{s=1}^m \alpha_s \sum_{j=1}^k \text{tr} \left(\sum_{i=1}^k w_i Z_{ij}^s (Y_j^s)^{-1} \right)^2 > 0,$$

since by the assumption for B , for at least one j , $\sum_{i=1}^k w_i Z_{ij}^s \neq 0$. \square

The rank of B can be calculated using the pairwise distances between q and p points and only in very special circumstances this rank will be less than k . More formally, if a random process chooses the points, then

$$P(\text{rank}(B) < k) = 0.$$

4.3 Examples and conclusions

Figure 5 shows interpolation between two *pmfs* of size 6 ($m = 2, k = 6$) applying $h_{\text{trln}2}$. We compare it to the linear and the square root interpolations. Square root interpolation, as suggested by the name, relies on the observation that for a *pmf* $f \in P_k^+$, $\sqrt{f} = (\sqrt{f^1}, \dots, \sqrt{f^k}) \in \mathbb{S}^k$. Then one finds

$$\hat{p} = \underset{p \in \mathbb{S}^k}{\text{argmin}} \sum_s \alpha_s d^2(p, \sqrt{f^s}) \text{ and sets } \hat{f}_{\text{sqrt}} = \hat{p}^2. \quad (12)$$

It is also informative to compare the Mean-Squared Error (MSE) between different interpolations. It is defined by

$$MSE(\hat{f}) = \sum_{s=1}^2 \alpha_s \sum_{i=1}^k (\hat{f}_i - f_i^s)^2. \quad (13)$$

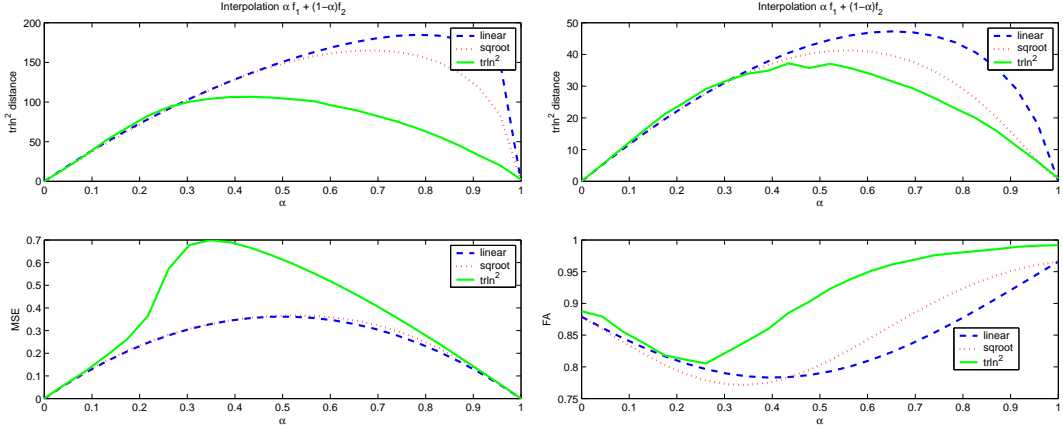


Figure 5: Two examples of interpolation of *pmfs* on \mathbb{S}^2 using h_{trln2} . The linear and square root (see (12)) interpolations are also given for reference. Top plots show H_{trln2} and H_{lik} for the three interpolations. Bottom plots show corresponding MSEs (see (13)) in the left and FAs (see (14)) in the right.

Linear and square root interpolations, by their nature, are very close in MSE, but very different from $\hat{f}_{trln2}(\alpha)$, which manifests the non-linear origin of the latter.

Another performance criteria relevant to the study of spherical data is the Fractional Anisotropy (FA). Let $\{\lambda_i\}_{i=1}^n$ be the eigenvalues of $\sum_{i=1}^k \vec{p}_i \vec{p}_i' f_i$, where \vec{p}_i are considered vectors in \mathbb{R}^3 (thus FA is defined only for distributions on \mathbb{S}^2). Then we define

$$FA(f) = \left\{ \frac{n}{n-1} \sum_{i=1}^n (\lambda_i - \bar{\lambda})^2 / \sum_{i=1}^n \lambda_i^2 \right\}^{1/2}. \quad (14)$$

Fractional Anisotropy measures a distribution concentration. The higher FA the more concentrated it is about particular axes. A uniform distribution has $FA = 0$. As we may expect the linear interpolation substantially reduces the FA index, h_{trln2} -based one however, is more conservative and manage to sustain higher FA. Preserving the concentration factor is of importance for processing ODFs in HARDI, and the empirical evidence for the good FA performance of h_{trln2} is encouraging.

A second set of examples in figure 6 illustrates interpolation based on the likelihood function, h_{lik} . As we showed, this choice guarantees the convexity

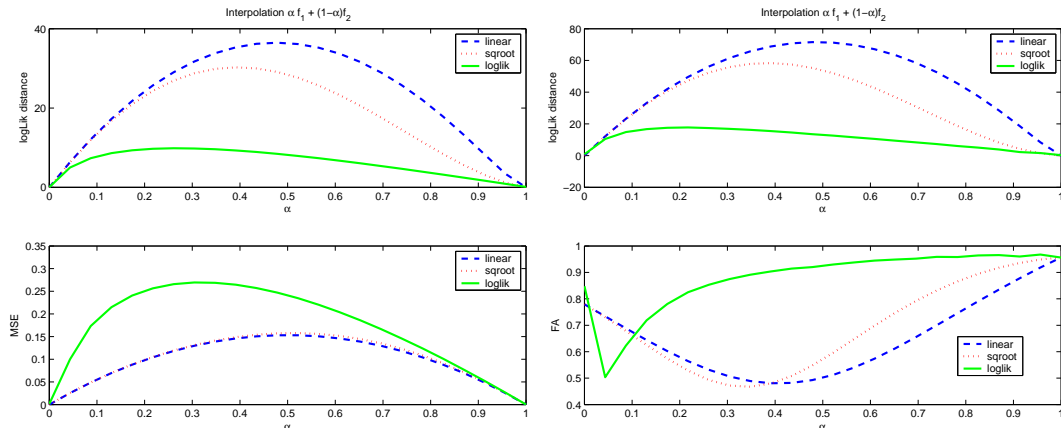


Figure 6: Two examples of interpolation of $pmfs$ on S^2 using h_{lik} . The linear and square root interpolations are also given for reference. Top plots show H_{lik} for the three alternatives. Bottom plots show corresponding MSEs in the left and FAs in the right.

of H_{lik} and thus the continuity of the optimal solution $\hat{f}_{lik}(\alpha)$.

The likelihood based interpolation \hat{f}_{lik} exhibits behaviour similar to that of \hat{f}_{trln2} . Again, it is very distinguished from the linear and the square-root one and tends to preserve the anisotropy.

5 Summary

The main goal of this article is to introduce covariance operator fields and provide some arguments showing their potential and usefulness.

There is a covariance field associated with any distribution on a Riemannian manifold. It defines a linear operator on the tangent space of each point on the manifold. By applying a similarity invariant to that operator field one can obtain a scalar field that represents the distribution. It reveals important spatial characteristics of the distribution. Similarity invariants can also be used for comparing and interpolating distributions.

We demonstrated several non-parametric procedures for solving a two-sample location problem on the sphere and showed how covariance operator fields can be used for locating observation points that maximize test performance.

We also implemented two non-linear procedures for interpolating distributions on the sphere and compared them to the linear and square-root

interpolations. The proposed approach is general enough to allow a great variety of choices and promises a good application potential.

6 Acknowledgements

We thank Vic Patrangenaru for the helpful comments and useful discussions. We also thank Paul Thompson from UCLA School of Medicine for providing us with a HARDI volume for research purposes.

References

- [1] Arsigny, V., Fillard, P., Pennec X., and Ayache, N. (2007) Geometric means in a novel vector space structure on symmetric positive-definite matrices. *SIAM Journal on Matrix Analysis and Applications*, 29(1):328-347.
- [2] Bhattacharya R. and Patrangenaru, V. (2003) Large Sample Theory of Intrinsic and Extrinsic Sample Means on Manifolds - I *The Annals of Statistics*, Vol.31(1), 1-29.
- [3] Bhattacharya R. and Patrangenaru, V. (2005) Large Sample Theory of Intrinsic and Extrinsic Sample Means on Manifolds - II *The Annals of Statistics*, Vol.33.
- [4] Bahlmann, C. (2006) Directional features in online handwriting recognition. *Pattern Recognition*, 39.
- [5] Batchelor, P., Moakher, M., Atkinson, D., Calamante, F., Connelly, A. (2005) A rigorous framework for diffusion tensor calculus. *Magn. Reson. Med.*, 53(1), 221-225.
- [6] Beran, R., and Fisher, N. (1998) Nonparametric comparison of mean directions or mean axes. *Ann Statistics*, Vol.26, 472-493.
- [7] M.P. Do Carmo. *Riemannian Geometry*, Birkhauser, Boston, 1992.
- [8] I. Chavel. *Riemannian Geometry: A Modern Introduction*, Cambridge University Press, 1993.
- [9] Chiang MC, Barysheva M, Lee AD, Madsen SK, Klunder AD, Toga AW, McMahon KL, de Zubicaray GI, Meredith M, Wright MJ, Srivastava A, Balov N, Thompson PM . Mapping Genetic Influences on Brain Fiber

Architecture with High Angular Resolution Diffusion Imaging (HARDI), ISBI 2008.

- [10] Dryden, I., Koloydenko, A., and Zhou, D., (2008) Non-Euclidean statistics for covariance matrices, with applications to diffusion tensor imaging. University of Nottingham, NG7 2RD, UK.
- [11] Fisher, R.A. (1953) Dispersion on a sphere. Proc. Roy. Soc. London Ser. A., 217, 295-305.
- [12] Fisher, N.I., Lewis, T., Embleton, B.J.J. Statistical analysis of spherical data. Cambridge University Press, 1987.
- [13] Fletcher, P. T., Joshi, S., (2007) Riemannian geometry for the statistical analysis of diffusion tensor data. Signal Processing, 87(2):250-262.
- [14] Fletcher, P. T., Joshi, S., Lu, C., Pizer, S. M. (2004) Principal geodesic analysis for the study of nonlinear statistics of shape. IEEE Transactions on Medical Imaging, 23(8), 9951005.
- [15] Forstner, W., Moonen, B. (1999) A Metric for Covariance Matrices. Stuttgart University.
- [16] Helgason, S., (1978) Differential Geometry, Lie Groups, and Symmetric Spaces. *Academic Press*. New York
- [17] Hollander, M., Wolfe, D., Nonparametric Statistical Methods. Wiley, 2nd, 1999.
- [18] Huchemann, S., Hotz, T., Munk, A., (2007) Intrinsic Shape Analysis: Geodesic PCA for Riemannian Manifolds Modulo Isometric Lie Group Actions, *Statistica Sanica*.
- [19] Karcher, H. (1977) Riemannian center of mass and mollifier smoothing, *Communications on Pure and Applied Mathematics*,30(5):504-541.
- [20] Kendall, D., (1984) Shape Manifolds, Procrustean metrics, and complex projective spaces. *Bull. London MATH Soc*,16:81-121.
- [21] Kendall, D., Barden, D., Carne, T., Le, H. (1999) Shape and Shape Theory Wiley, New York.

- [22] Kent, J. (1982) The Fisher-Bingham distribution on the sphere. *J. Royal Stat Soc.* 44, 7180.
- [23] Kent, J.T., Hamelryck, T. Using the Fisher-Bingham distribution in stochastic models for protein structure. In S. Barber, P.D. Baxter, K.V.Mardia, R.E. Walls (Eds.), *Quantitative Biology, Shape Analysis, and Wavelets*, pp. 57-60. Leeds, Leeds University Press, 2005.
- [24] Krieger L, N. C., Juul J., D., Conradsen, K. (1994) On the statistical analysis of orientation data. *Acta Cryst.*, A50, 741-748
- [25] John M. Lee. *Introduction to Smooth manifolds*, 2000.
- [26] Mardia, K. *Directional statistics and shape analysis*. Research Report STAT95/24, University of Leeds.
- [27] Mardia K.M., Jupp P. (2000) *Directional Statistics* (2nd). John Wiley and Sons Ltd.
- [28] Mardia K.M., Taylor C.C. Subramaniam, G.K. (2007) Protein Bioinformatics and Mixtures of Bivariate von Mises Distributions for Angular Data. *Biometrics*, 63, 505-512
- [29] Ohara, A., Suda, N., Amari, S. (1996) Dualistic Differential Geometry of positive definite matrices and its applications to related problems. *Linear Algebra and Its Applications* 247:31:53.
- [30] Pennec. X., Fillard, P., Ayache, N (2006), A Riemannian framework for tensor computing. *Int. J. Computational Vision*, 66(1):41-66.
- [31] Pennec. X. (1999) Probabilities and statistics on Riemannian manifolds: basic tools for geometric measurements. *IEEE Workshop on Nonlinear Signal and Image Processing*.
- [32] Srivastava, A., Jermyn, I., Joshi, S. (2007) Riemannian Analysis of Probability Density Functions with Applications in Vision *IEEE Conference on Computer Vision and Pattern Recognition (CVPR)*.